Comparing Prior and Learned Time Representations in Transformer Models of Timeseries

Natalia Koliou*
Tatiana Boura*
Stasinos Konstantopoulos
{nataliakoliou,tatianabou,konstant}@iit.demokritos.gr
Institute of Informatics and Telecommunications,
NCSR 'Demokritos'
Ag. Paraskevi, Greece

George Meramveliotakis
George Kosmadakis
{gmera,gkosmad}@ipta.demokritos.gr
Institute of Nuclear & Radiological Sciences and
Technology, Energy & Safety,
NCSR 'Demokritos'
Ag. Paraskevi, Greece

ABSTRACT

What sets timeseries analysis apart from other machine learning exercises is that time representation becomes a primary aspect of the experiment setup, as it must adequately represent the temporal relations that are relevant for the application at hand. In the work described here we study wo different variations of the Transformer architecture: one where we use the fixed time representation proposed in the literature and one where the time representation is learned from the data. Our experiments use data from predicting the energy output of solar panels, a task that exhibits known periodicities (daily and seasonal) that is straight-forward to encode in the fixed time representation. Our results indicate that even in an experiment where the phenomenon is well-understood, it is difficult to encode prior knowledge due to side-effects that are difficult to mitigate. We conclude that research work is needed to work the human into the learning loop in ways that improve the robustness and trust-worthiness of the network.

CCS CONCEPTS

• **Computing methodologies** → **Neural networks**; **Artificial intelligence**; *Supervised learning*; • **Mathematics of computing** → *Time series analysis*.

1 INTRODUCTION

What sets apart timeseries analysis from other machine learning exercises is taking into account the sequence as well as, in most cases, the temporal distance between observations. This makes the representation of time a primary aspect of the experiment setup,

*Both authors contributed equally to this research.

as it must be adequate for representing the temporal relations that are relevant for the application at hand.

To elaborate on the various considerations that need to be addressed, first consider that one cannot assume fully observed, uniformly sampled inputs as there might be gaps in the data, varying sampling rates, and (for multivariate timeseries) misalignment between the time steps of the different variables. This dictates a representation that allows time differences to be computed, so that (for example) September 2023 is 'closer' to January 2024 than it is to September 2022. Simple timestamps allow this but do not capture periodicity: Consider, for instance, an application with seasonal periodicity where September 2023 is 'closer' to September 2022 than to January 2024.

There is a rich relevant literature in both signal processing and in non-parametric statistics, as well as in adapting AI/ML approaches to timeseries processing when facing irregularly sampled and/or sparse data. In particular, deep learning approaches that utilize recurrent networks based on Gated Recurrent Units (GRUs) [1], Long Short-Term Memory networks (LSTMs) [2, 3], and ODE-RNNs [4] have shown promising results. In the work described we focus on deep learning methods as well, but specifically on adapting *Transformer* models to timeseries analysis. We will first present how the relevant literature handles the representation of time when applying Transformer models to timeseries (Section 2) and then proceed to propose an alternative representation that is expected to out-perform the original representation for our specific application on predicting the energy output of solar panels (Section 3). We close with giving and discussing comparative experimental results (Section 4) and conclusions and future work (Section 5).

2 BACKGROUND

Unlike recurrent and differential equation-based architectures which process inputs sequentially, Transformers [6] expect the complete time-series as input and use the *attention* mechanism to look for relationships between all inputs simultaneously. This has the side-effect that the temporal order is no longer implied by the order in which the inputs are presented to the network, so that input vectors must be augmented with features that represent time. But this also creates the opportunity to use *time embeddings* that represent temporal information in a way that encodes prior knowledge about the data.

The most characteristic example is periodicity. When the data is known or suspected to exhibit periodicity, *absolute positional encoding* [7] encodes time as two features: the sine and the cosine

Natalia Koliou, Tatiana Boura, Stasinos Konstantopoulos, George Meramveliotakis, and George Kosmadakis

of the raw timestamp. This representation allows the Transformer to refer to both absolute times (since the combination of sine and cosine maps to a single position on the trigonometric circle) and to a representation where all (for instance) peak positions have the same feature value. Referring back to our previous example, remember how we want September 2022 and September 2023 to be on a similar or identical time from the periodic perspective, but not from the linear-time perspective. The Transformer will then have the flexibility to weigh these features in accordance with the phenomenon being modeled.

The meaningful and successful usage of pre-computed time features requires expert knowledge of the application domain and the periodicities that make sense for the phenomenon being modeled. In other words, it adds upon the inductive bias of the algorithm.

As expected, a line of research emerged that aims to automatically acquire the time representation from the data. The *multi-time attention network (mTAN)* [5] is a Transformer model enhanced with a time-attention module. This module learns temporal patterns by leveraging a trainable embedding function $\phi(t)$ that maps time t (scaled to 0..1) to a vector of length d.

This vector has one linear element that captures the linear progression of time and $d - 1$ sinusoidal elements that capture different periodicities as frequency/phase pairs. Formally, the embedding function is:

$$\phi_i(t) = \begin{cases} \omega_0 t + \alpha_0, & \text{if } i = 0, \\ \sin(\omega_i t + \alpha_i), & \text{if } 0 < i < d \end{cases} \tag{1}$$

where ω_i and α_i are the learnable parameters.

In concrete neural network terms, this is implemented as one linear layer for ω_0, α_0 and one linear layer with a sine activation function for all other ω_i, α_i. More precisely, it is implemented with multiple such structures, one for each attention head. It should be noted at this point that for the matrix multiplications to work out, this modeling has the side-effect that d must be the same as the dimensionality of the output vector.

This modeling gives the Transformer the flexibility to search for the period/phase pairs that best capture the periodicities implied by the data. Only minimal bias is introduced, namely that time is structured as a sine/linear pair.

3 REPRESENTING TIME

In order to experiment with time representations and the effect they have on the quality of the learned model, we have assumed an application where we need to predict the energy output of solar thermal collectors based on external conditions. More detailed information about the application and the data is provided in Section 4, and for the purposes of the current discussion it suffices to mention that the input variables are solar radiation and external temperature, which exhibit the obvious daily and annual periodicities.

We have noted however, that solar radiation behaves in a way that is not captured by sinusoidal functions. While these functions represent well the similarity between the same time on a different day, as well as the similarity between early morning and late afternoon, they fail to represent the fact that the whole of the night-time is the same and (as far as solar radiation is concerned) it makes no difference if the time is 10pm or 24am. We have, therefore, thought
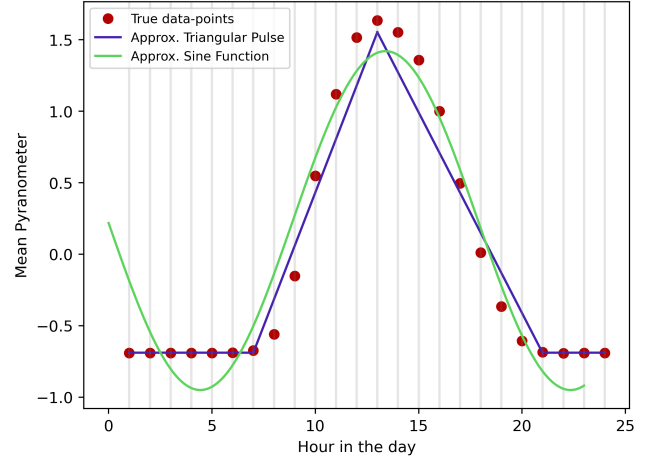

Figure 1: Hourly mean pyranometer values (red) and their function approximations, triangular pulse (blue) and sinusoidal function (green).

that a triangular spike will be a better representation than a sine. This is further corroborated by the data shown in Figure 1, showing pyranometer (solar radiation) values aggregated to 1h intervals and averaged through the year, and the best approximation that can be achieved by the sine function and by the triangular spike.

Based on the argument above, we have defined the four alternative time embeddings presented below.

3.1 Triangular Pulse & Linear

The first embedding is a season-modulated triangular pulse/linear pair. The base and peak of the triangular pulse is not the same for each day, but is calculated so that the pulse will start at sunrise, peak at noon, and end at sunset. This represents that solar radiation at noon is distinct from all other times during day, one hour before noon is similar to one hour after noon, and so on until sunrise/sunset. Outside the base of the pulse, all times are represented by the same value of 0.01 to denote that the distinction between them is not important.[1]

As for the linear function, it provides a straightforward method for ensuring the uniqueness of timestamps within the representation. By mapping each timestamp to a unique value, we establish clear distinctions between different time points. Unlike the periodicity of the triangular pulse, the linear function spans the entire range of timestamps, from the earliest to the latest, using both date and time components. This continuous representation does not reset daily but maps the entire period linearly, ensuring a unique value for each timestamp based on its position in the overall time span.

The second embedding is similar to the one above, but the pulse is fixed to start at 7am, peak at 1pm, and end at 9pm regardless of the date. This simpler embedding is included in order to be able to see if the more complex approach above has added value or there is no significant loss in accuracy when using fixed parameters.

---

[1]This value is set to 0.01 instead of 0 to satisfy a technical requirement of the implementation.
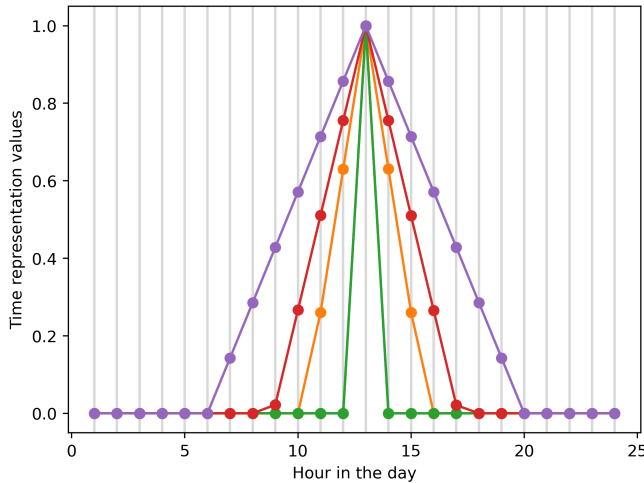
Figure 2: Examples of learned time representation features with a learnable triangular pulse. The five illustrated time features come from the same testing sample and highlight the capability of the model to learn (non-)isosceles pulses with different bases.

3.2 Sinusoidal

The third embedding follows the absolute positional encoding literature and consists of two sine/cosine pairs, one pair computed from the month of the year and one pair computed from the hour of the day. Sine and cosine capture cyclical patterns effectively, and by combining the hour and the month embedding we guarantee that the Transformer has the means to model daily and annual periodicities and also to refer to absolute timepoints if the data prove this useful.

To find the appropriate phase shift and period, we argue as follows: To represent the daily cycle we need our sine wave to peak at noon. We aim for noon to be distinct, while the remaining timestamps should exhibit symmetrical correlation. To achieve this, observe how a period of 12 for hours and 24 for months, with a zero shift, will work as expected. Naturally, the cosine must be parameterized with identical phase and period to maintain the property that the sine/cosine pair uniquely refers to a point in the trigonometric circle.

3.3 Sine & Sawtooth

The fourth and final embedding consists of a sine and a sawtooth function. Just like in the sinusoidal embedding, we also use the sine wave with the same parameters (shift, period) to express correlation among timestamps. However, when it comes to expressing uniqueness, we considered using a sawtooth wave instead of a cosine wave, to observe whether any noticeable changes might take place. Unlike the linear function used in the triangular pulse embeddings which spans the entire range of timestamps, the sawtooth wave resets to 0 output after each day. The sawtooth wave parameters (shift, period) are set to (6, 6) for hours and (12, 12) for months to scale the output values for both cases within [-1, 1].

3.4 Learned Time Representations

As mentioned in the Background, the idea behind the *mTAN* is to learn periodic features with a sinusoidal representation. We have argued that, for our application, a triangular pulse for representing the non-linear features may be a better fit. Thus, we altered the activation function of the presented model to convert the linear layer to a triangular pulse.

Our first attempt at creating such a function involved using a triangular function with a fixed base. In this case, the start and end of the pulse corresponded to the hours when difference of the solar output peaked (7 AM and 9 PM respectively). This approach was not fruitful, as the model was not given the opportunity to learn the periodic representations.

Naturally, we then focused on learning the base of the pulse. Choosing 1 PM as the peak of the pulse, the two most straightforward approaches we implemented were: (a) splitting the time vector and then using the hours where the absolute difference of the elements in the learned time vector is the largest as the start and end of the pulse; and (b) splitting the time vector and then using the hours where the elements themselves in the learned time vector have the absolute largest values as the start and end of the pulse. However, both implementations failed to learn any meaningful form of pulse and remained fixed on the initial time parameters.

The approach that successfully achieved the task of learning different triangular pulses was an engineering one. It emerged from the idea that the non-linear function itself should be simple in terms of numerical computation and traceability, since the previous, more complex approaches were not suitable for the task. The idea is described as follows: we first calculate the absolute difference of each value in the time vector of each representation of size d and the value of the 13th element of this representation (corresponding to 1 PM). Then we compute the 25th percentile of these differences and replace each difference $dist_{ij}$ with zero if it is less than the percentile value v_i of the corresponding representation i, and with $1 - \frac{dist_{ij}}{v_i}$ otherwise. Figure 2 presents a few example triangular pulse time representations learned from employing this approach.

4 EXPERIMENTS AND RESULTS

4.1 Experimental setup

Our data was collected from a pilot building at NCSR 'Demokritos'. The pilot building features solar thermal collectors used to experiment with how to most efficiently control heating systems (solar, heat pump, etc.) to achieve satisfactory space heating, satisfy hot water demand, and minimize electric power consumption. The machine learning task associated with this application is to predict solar power production from variables reflecting external conditions, namely solar radiation and external temperature. The output of the model is not specific power in terms of kWh, but a label that characterizes power production as being in one of five classes, defined based on expected demand.

Based on the above, the machine learning task is to transform a multi-variate timeseries of external conditions aggregated into one-hour intervals, into a timeseries of power production levels (the five-class labeling schema mentioned above). The dataset has a moderate amount of gaps due to the sensors occasionally giving erroneous,

Natalia Koliou, Tatiana Boura, Stasinos Konstantopoulos, George Meramveliotakis, and George Kosmadakis

Table 1: Evaluation results for the classification task using prior and learned time representations. Each model was trained using six different initialization seeds, and the final metrics are composed from the aggregation (mean and standard deviation) of the results from these trained models.

Metric	Prior Time Representations				Learned Time Representations	
	tr. pulse & linear †	fixed tr. pulse & linear †	sine & cosine ‡	sine & sawtooth ‡	sine & linear †	tr. pulse & linear †
Precision (Micro)	0.835 ± 0.017	0.823 ± 0.013	$\mathbf{0.866} \pm 0.010$	0.860 ± 0.004	$\mathbf{0.842} \pm 0.009$	0.778 ± 0.010
Recall (Micro)	0.835 ± 0.017	0.823 ± 0.013	$\mathbf{0.866} \pm 0.010$	0.860 ± 0.004	$\mathbf{0.842} \pm 0.009$	0.778 ± 0.010
F-score (Micro)	0.835 ± 0.017	0.823 ± 0.013	$\mathbf{0.866} \pm 0.010$	0.860 ± 0.004	$\mathbf{0.842} \pm 0.009$	0.778 ± 0.010
Precision (Macro)	0.650 ± 0.027	0.629 ± 0.012	$\mathbf{0.679} \pm 0.025$	0.666 ± 0.009	$\mathbf{0.647} \pm 0.012$	0.582 ± 0.015
Recall (Macro)	0.715 ± 0.033	0.673 ± 0.015	$\mathbf{0.722} \pm 0.024$	0.721 ± 0.026	$\mathbf{0.694} \pm 0.023$	0.621 ± 0.016
F-score (Macro)	0.663 ± 0.030	0.632 ± 0.013	$\mathbf{0.689} \pm 0.019$	0.676 ± 0.016	$\mathbf{0.646} \pm 0.019$	0.571 ± 0.013
Precision (Weighted)	0.884 ± 0.010	0.876 ± 0.006	0.894 ± 0.009	$\mathbf{0.895} \pm 0.004$	$\mathbf{0.892} \pm 0.005$	0.867 ± 0.007
Recall (Weighted)	0.835 ± 0.017	0.823 ± 0.013	$\mathbf{0.866} \pm 0.010$	0.860 ± 0.004	$\mathbf{0.842} \pm 0.009$	0.778 ± 0.010
F-score (Weighted)	0.853 ± 0.013	0.842 ± 0.008	$\mathbf{0.876} \pm 0.009$	0.872 ± 0.004	$\mathbf{0.860} \pm 0.007$	0.812 ± 0.009

†: input being sec/min/hour/day/month/year   ‡: input being month/hour
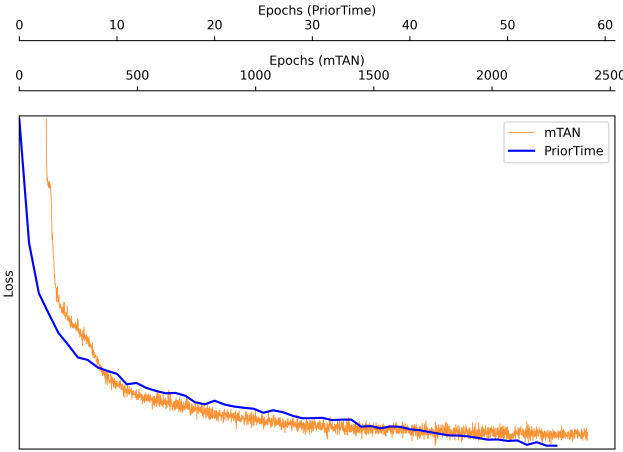
Figure 3: Normalized training loss progression for each model. The models presented are the best-performing models across different time representations (prior and learned).

out-of-range readings which are removed. The dataset exhibits the obvious daily periodicity, and also exhibits a non-periodic trend. The non-periodic trend is in reality seasonal periodicity, but since we have used the data from 10 months it appears to the machine learning task as a non-periodic trend.[2]

To apply the prior time representation we implemented a Transformer with an encoder, a decoder, and a classifier, in that order. We refer to this architecture as *PriorTime* in the results presented below. The encoder maps the input into a latent representation, the decoder reconstructs it preserving the original dimensionality of its features, and the classifier (a single linear layer) outputs a probability distribution over the five labels. To apply the learned time representation, we used the *mTAN* architecture, where the decoder is the same single-layer linear classifier. Figure 3 give the training

[2]Available at https://zenodo.org/records/12818885

loss from training these models. The complete experimental setup is also published.[3]

4.2 Classification results and discussion

To evaluate the performance of our models on the classification task, we compared both the *PriorTime* and *mTAN* models across different time representations. Our evaluation criteria included various performance metrics such as precision, recall, and F1-score, as shown in Table 1.

The *PriorTime* model was trained and tested using four different time representations: triangular pulse & linear, fixed triangular pulse & linear, sine & cosine, and sine & sawtooth. Among these representations, the sine & cosine approach consistently demonstrated the strongest performance. The sine & sawtooth representation approached the results achieved by sine & cosine; however, it only outperformed once, and the difference was not significant. Concerning the two triangular pulse/linear representations, they exhibited the weakest performance overall, with the fixed variation performing slightly worse than the season-modulated one. This was not surprising, as we expected the more informed time representation to give better results.

The second point is that the sine representations consistently outperform the triangular ones in both settings (prior and learned), despite the fact that the triangular pulse is more precise when it comes to making similar times have similar inputs (solar radiation and temperature), as already discussed in the beginning of Section 3. We believe that this is due to the fact that the identical close-to-zero values outside the base of the pulse hinder back-propagating loss to the linear layer that feeds the sine/triangular activation function.

When these two points are put together, they imply that (a) the first linear layer is capable of managing both seasonal variation and the daily periodicity by properly weighting the inputs of the activation functions; (b) (almost) zeroing-out inputs hinders back-propagation; and (c) having an activation function that dynamically changes to model the unique characteristics of each day individually enhances convergence.

[3]See guide under `time_representations/installation` at the `AINST-2024` branch of repository https://github.com/data-eng/navgreen and also directly accessible at https://github.com/data-eng/navgreen/releases/tag/AINST-2024

(a) Initial feature representation


(b) Final feature representation
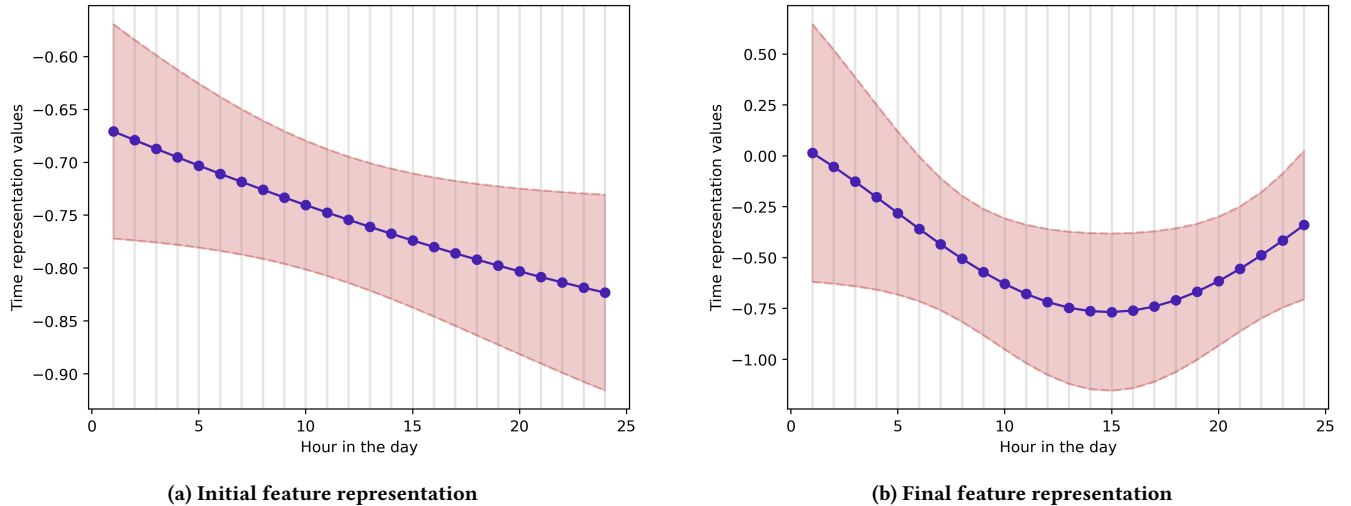
Figure 4: Example of the learning progress of a sine time feature. Both figures illustrate the time representation of the test examples by aggregating them per time-feature using the mean and standard deviation. The left figure shows the feature before the learning process starts, while the right one shows the final learned feature. The learned time representation is meaningful since it distinguishes midday and has similar values for hours with similar accumulated daylight.

4.3 Discussion of the Learned Time Representations

As noted in Section 2, we are bound by the model's architecture to learn $n-1$ periodic and 1 non-periodic feature representations from our data, with n being the number of the final output points of the time series (in our case, 24).

When subjecting the periodic time representation to be a triangular pulse, the model starts from very narrow pulses and then proceeds to learn a combination of those, as presented previously in Figure 2. On the other hand, when we define the periodicity as a sine function, the initial weight initialization (which sets the weights to very small values) makes the initial representations a very short part of the sinusoidal curve (so short that visually appears as linear in our graphs). The model then learns to scale the time vectors to model more meaningful time representations. An example of this behavior is presented in Figure 4.

However, one might wonder: are all of the 23 learned time representations meaningful? Since it is hard to track the influence of every representation on the classification task, we can only speculate. In Figure 5 are demonstrated all the periodic sine features, grouped by their similarity. Most time features fall into the first three groups. The last three groups, which only include one representation each, seem to be the most explainable regarding our knowledge of the domain. They capture larger periods that lead to the numerical correlation of different hours in a day. We believe that these are the most important features on which the model's prediction relies and also that when it started to learn these features, it neglected the others and assigned smaller weights to them. To substantiate this assertion we illustrate in Figure 6 the corresponding groups at the start of the learning process. It can be claimed that the first three groups exhibit minimal change, whereas the last three change visibly.

To model the time points for each example, we normalized each timestamp using the Unix timestamps from our data's date range. The resulting time points range from 0 to 1, but within a daily sample, the hourly time points vary slightly. The Transformer's architecture utilizes the key/value/query formulation [6]. The query is the information that is being looked for, the key is the context or reference, and the value is the content that is being searched. In the context of *mTAN*, the initial keys are the time points and the initial queries are vectors with values equally distributed from 0 to 1. Both of these terms are then passed through the same learnable time layers. Since, initially, the keys and the queries have a different order of magnitude it is expected that either the model will increase the magnitude of the keys or decrease the magnitude of the queries. Through our experiments we discovered that the former occurs. As presented in Figure 7 the smaller key values correspond to a smaller part of the sine wave, whereas the larger query values cover a larger part of the sine wave (Figure 8).

To further evaluate our claim, we modified the time point creation so that both queries and keys have the same values. To do so, we assigned each time point referring to an hour in a day its normalized index by dividing it with the total number of hours in a day. As expected, the learned representation then was the same for both keys and queries, as illustrated in Figure 9. Comparing them to the previously learned representations in Figures 7 and 8, the evaluation of the keys has indeed scaled up, while the evaluation of the queries has not changed drastically.

The main reason we opted for normalizing the time steps using UNIX time was that it slightly performed better for the classification task. We believe that this is the case because when normalizing the time points considering only the hour, we lose any other characteristic that relates to the progression of time. This further corroborates that (as we extensively stressed earlier) the non-periodical features are crucial for our application.

Natalia Koliou, Tatiana Boura, Stasinos Konstantopoulos, George Meramveliotakis, and George Kosmadakis

(a) Group 1 (7 time representations)   (b) Group 2 (9 time representations)   (c) Group 3 (4 time representations)

(d) Group 4 (1 time representation)   (e) Group 5 (1 time representation)   (f) Group 6 (1 time representation)
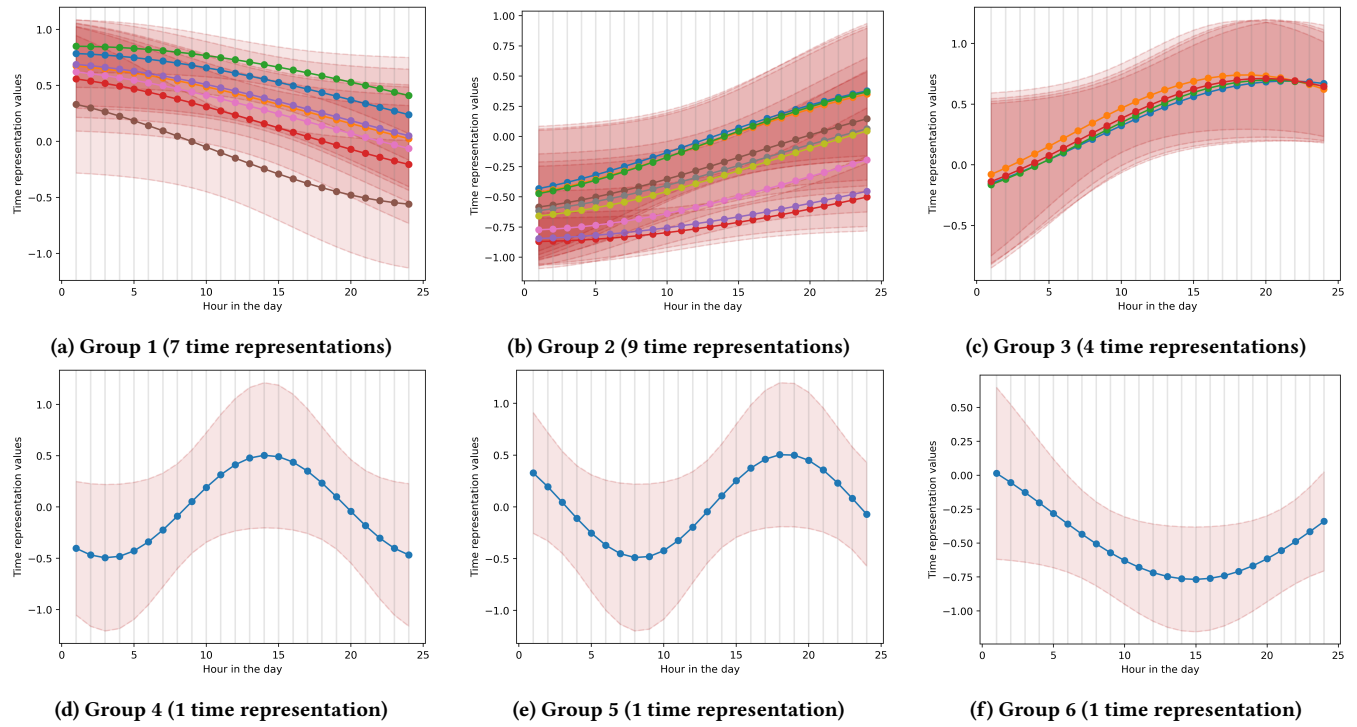
Figure 5: Learned sine time representations grouped by their similarity. Each figure is comprised of the aggregated representations computed on the testing data (mean and standard deviation of each time-feature). The top three figures gather the majority of the features, whereas the bottom three include only one feature each.

(a) Group 1   (b) Group 2   (c) Group 3

(d) Group 4   (e) Group 5   (f) Group 6
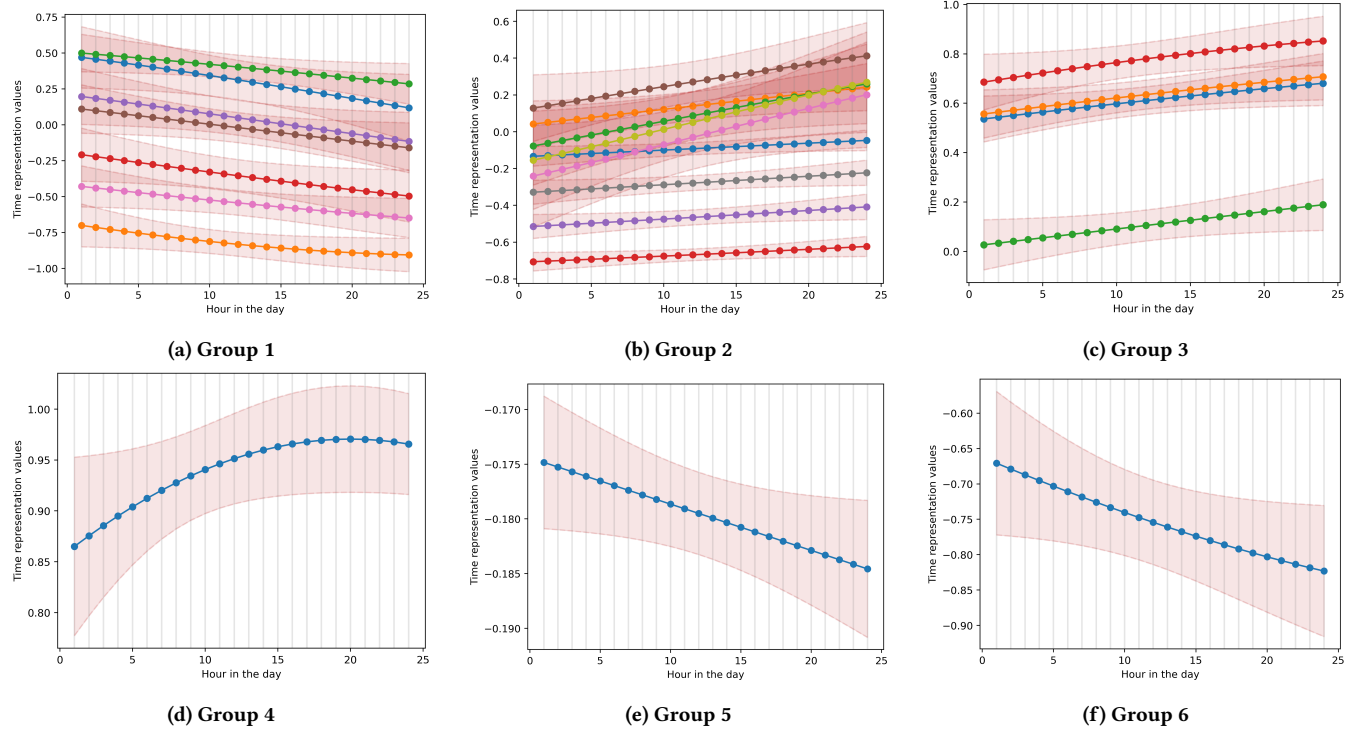
Figure 6: Initial values of the groups of the sine time representations.
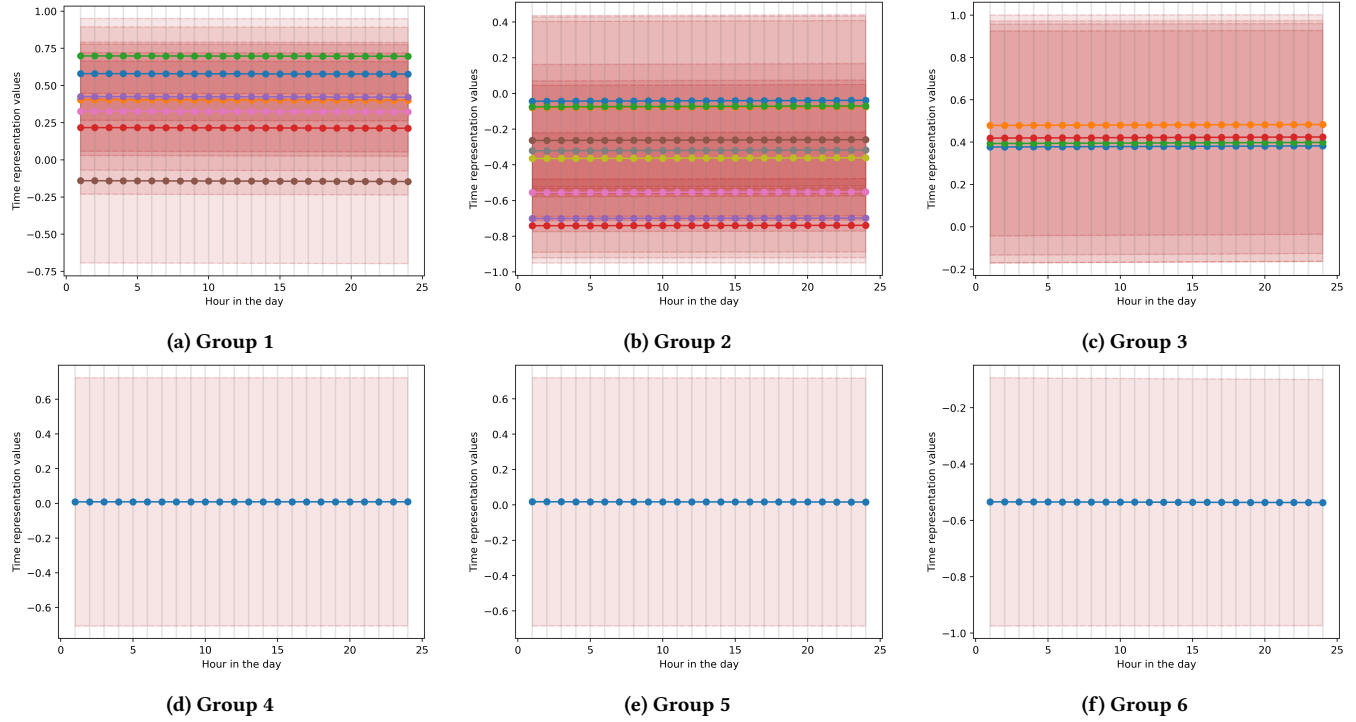
Figure 7: Learned sine time representations on the keys of the test data. The illustrated representations occurred when the keys and queries had different orders of magnitude.
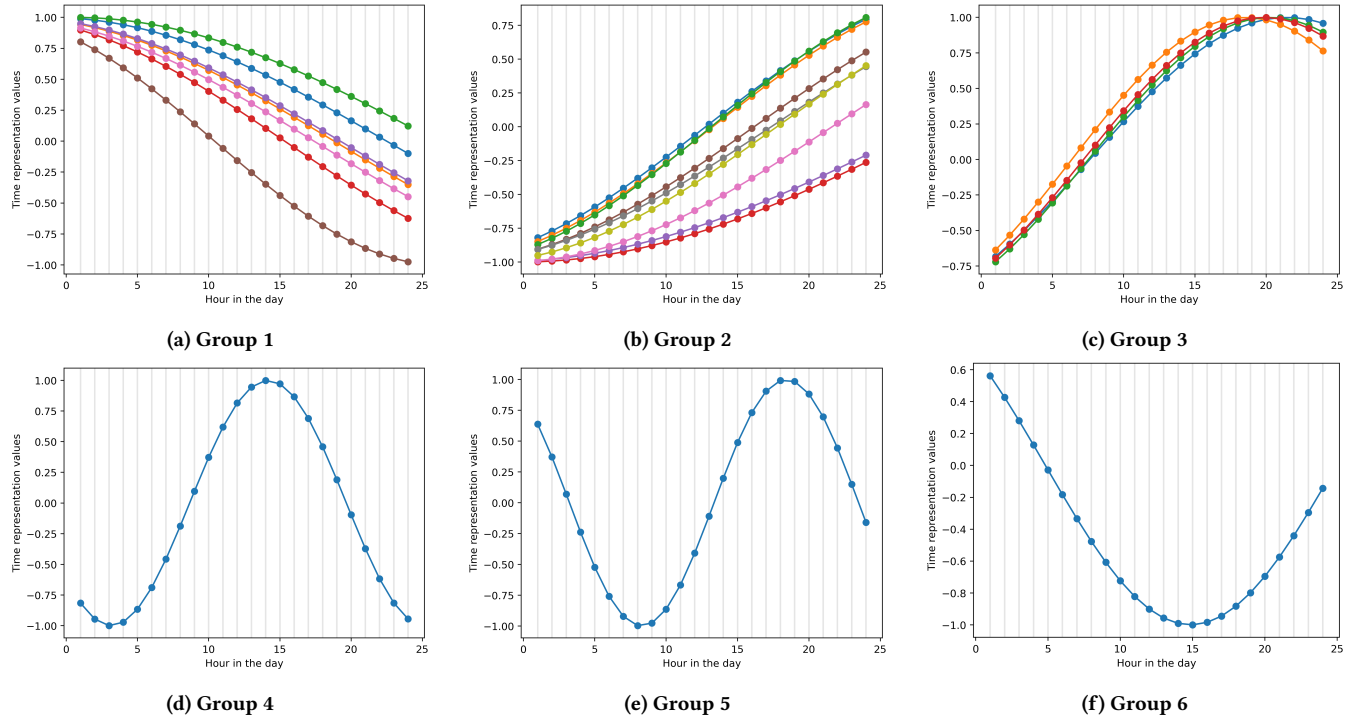

Figure 8: Learned sine time representations on the queries of the test data. The illustrated representations occurred when the keys and queries had different orders of magnitude.
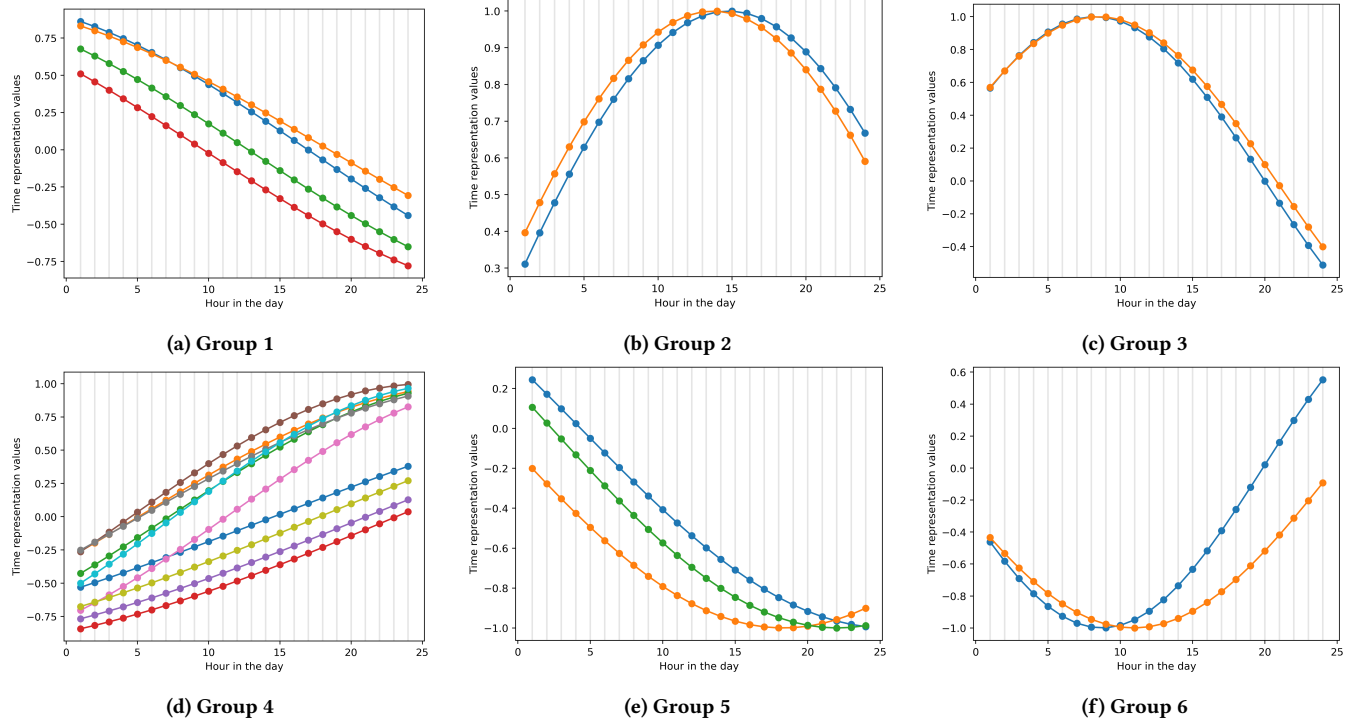
Figure 9: Learned sine time representations on the keys and queries of the test data. The illustrated representations occurred when the keys and queries had the same order of magnitude.

5 CONCLUSIONS

We studied the impact of time embeddings when applying Transformer models to timeseries analysis, and specifically the impact of using a very informed, application-specific time representation, a generic sinusoidal representation known to capture periodic phenomena well, and a method for learning the parameters that best fit either of these two to the specific dataset at hand.

Our experiments concluded that Transformers (and DNNs in general we could argue) are not very amenable to over-engineering the time representation due to side-effects that are difficult to mitigate. This can be seen as a negative quality in applications such as ours where there is extensive prior knowledge on a well-studied phenomenon, but can also be construed as a positive quality as the network was able to 'discover' the knowledge we were trying to convey. Especially the comparison between the sinusoidal prior and learned representations is very promising in this respect, at the maximally-flexible *mTAN* network recovered almost all the accuracy of the prior-time sinusoidal network.

A second level of analysis delved into the nature of the features that *mTAN* learned. This analysis has demonstrated the ability of the linear layer - sinusoidal activation function architecture to very closely approximate the clearly non-smooth behavior discussed in Section 3 and shown in Figure 1.

It should, however, be noted that our analysis was restricted to what we could indirectly observe by trying out different parameterizations and speculating based on our understanding of how the network is trained. Besides any general advancements in

methodologies for explaining neural networks, this also showed us a path for future work specifically targeting *mTAN*. Since one of the hindrances was that we were unable to observe the effect of each feature due the distributed nature of the classifier, we would have liked to systematically explore the effect of incrementally increasing the number of features and observing which features gets learned (interpreted as, is the most impactful for reducing loss), which is learned second and so on. However, the linear algebra behind *mTAN* ties the dimensionality of the feature representation to the dimensionality of the input, as we cannot de-couple the encoding of periodicity and the encoding of linear time. Since (as argued above) linear time is critical for performance, we are stuck with a pre-defined dimensionality for the sine features as well.

Our envisaged future research is to re-work the linear algebra of the *mTAN* so that we can de-couple the encoding of the periodic and linear time representation, allowing to have only the latter be constrained by the dimensionality of the input. In the specific experiment presented here, this would translate to a better understanding of what happens when we inform the Transformer of the bias we want to apply regarding periodicities. Which, in its turn, is expected to lead to methods for affording the human operator intuitive and effective control of the network.

ACKNOWLEDGMENTS

REFERENCES

[1] Zhengping Che, Sanjay Purushotham, Kyunghyun Cho, David Sontag, and Yan Liu. 2018. Recurrent Neural Networks for Multivariate Time Series with Missing Values. *Scientific Reports* 8 (04 2018). Issue 1.

[2] Daniel Neil, Michael Pfeiffer, and Shih-Chii Liu. 2016. Phased LSTM: Accelerating Recurrent Network Training for Long or Event-based Sequences. In *Advances In Neural Information Processing Systems*. 3882–3890.

[3] Trang Pham, Truyen Tran, Dinh Phung, and Svetha Venkatesh. 2017. Predicting healthcare trajectories from medical records: A deep learning approach. *Journal of Biomedical Informatics* 69 (2017), 218–229.

[4] Mona Schirmer, Mazin Eltayeb, Stefan Lessmann, and Maja Rudolph. 2022. Modeling Irregular Time Series with Continuous Recurrent Units. In *Proceedings of the 39th International Conference on Machine Learning, 17-23 Jul 2022*, Vol. 162.

[5] Satya Narayan Shukla and Benjamin Marlin. 2021. Multi-Time Attention Networks for Irregularly Sampled Time Series. In *International Conference on Learning Representations*.

[6] Ashish Vaswani, Noam Shazeer, Niki Parmar, Jakob Uszkoreit, Llion Jones, Aidan N Gomez, Ł ukasz Kaiser, and Illia Polosukhin. 2017. Attention is All you Need. In *Advances in Neural Information Processing Systems*, I. Guyon, U. Von Luxburg, S. Bengio, H. Wallach, R. Fergus, S. Vishwanathan, and R. Garnett (Eds.), Vol. 30. Curran Associates, Inc.

[7] Qingsong Wen, Tian Zhou, Chaoli Zhang, Weiqi Chen, Ziqing Ma, Junchi Yan, and Liang Sun. 2023. Transformers in Time Series: A Survey. In *Proceedings of the Thirty-Second International Joint Conference on Artificial Intelligence, Survey Track. Macao, 19–25 August 2023.* https://doi.org/10.24963/ijcai.2023/759